IFIC/16-41

Scalar-mediated double beta decay and LHC

L. Gonzales,* J.C. Helo,† and S.G. Kovalenko‡
Universidad Técnica Federico Santa María,
Centro-Científico-Tecnológico de Valparaíso,
Casilla 110-V, Valparaíso, Chile

M. Hirsch§
AHEP Group, Instituto de Física Corpuscular – C.S.I.C./Universitat de València
Edificio de Institutos de Paterna, Apartado 22085, E–46071 València, Spain

arXiv:1606.09555v1 [hep-ph] 30 Jun 2016

Abstract

The decay rate of neutrinoless double beta ($0\nu\beta\beta$) decay could be dominated by short-range diagrams involving heavy scalar particles ("topology-II" diagrams). Examples are diagrams with diquarks, leptoquarks or charged scalars. Here, we compare the discovery potential for lepton number violating signals at the LHC with constraints from dijet and leptoquark searches and the sensitivity of $0\nu\beta\beta$ decay experiments, using three example models. We note that already with 20/fb the LHC will test interesting parts of the parameter space of these models, not excluded by current limits on double beta decay.

Keywords: double beta decay; neutrino masses and mixing; LHC

*Electronic address: lorena.gonzalez@alumnos.usm.cl
†Electronic address: juan.heloherrera@gmail.com
‡Electronic address: Sergey.Kovalenko@usm.cl
§Electronic address: mahirsch@ific.uv.es

I. INTRODUCTION

From the theoretical point of view, neutrinoless double beta decay ($0\nu\beta\beta$) can be written as a dimension-9 operator:

$$\mathcal{O}^{0\nu\beta\beta} = \frac{c_9}{\Lambda^5_{LNV}} \bar{u}\bar{u}dd\bar{e}\bar{e}. \tag{1}$$

Here, Λ_{LNV} is the scale of lepton number violation (LNV). Many beyond the standard model contributions to this operator have been discussed in the literature, for a review see [1]. Contributions to the decay rate of $0\nu\beta\beta$ decay can be classified as (i) neutrino mass mechanism; (ii) long-range [2] and (iii) short-range contributions [3]. [1]

Particularly interesting is the possibility that all beyond-standard-model particles, appearing in the ultra-violet completions of this operator, are heavy. This corresponds to the short-range part of the $0\nu\beta\beta$ decay amplitude. In this case, with the current sensitivities of $0\nu\beta\beta$ decay experiments [6, 7] of the order of roughly $\mathcal{O}(10^{25} - 10^{26})$ yr, one probes mass scales in the range $\Lambda_{LNV} \sim (1-3)$ TeV - exactly the range of energy explored at the LHC.

A list of all possible decompositions of eq. (1) has been found in [8]. Models fall into two classes, called topology-I (T-I) and topology-II (T-II), see fig. (1). In this figures outside lines correspond to the six fermions appearing in eq. (1) , while the internal particles can be scalars, vectors or fermions. Just to mention one example for T-I and T-II each: In left-right (LR) symmetric models, right-handed gauge bosons (W_R) and neutrinos (N_R) appear in T-I as $W_R - N_R - W_R$ exchange [9, 10], while a T-II type diagram can appear as $W_R - \Delta_R^{\pm\pm} - W_R$ exchange [11] in LR models with right-handed triplets (Δ_R).

The classical LNV signal searched for at the LHC is two same-sign leptons plus jets ($lljj$), first discussed as a possible signal for left-right symmetric models in [12], see also [13]. This signal is generated from the T-I diagram with right-handed neutrinos. The doubly charged scalar can be searched via vector-boson-fusion, see for example [14, 15]. This corresponds to the T-II diagram mentioned above. VBF gives the same final state (lljj), but has different kinematics. We mention in passing that also di-lepton searches can be used to put bounds on LR models [16].

Both ATLAS and CMS have published results for run-I of the LHC. CMS [17] observed an excess in the electron sample around $m_{eejj} \simeq 2$ TeV,[2] but no excess in the muon sample. CMS interprets the excess as a statistical fluctuation. ATLAS used 20.3/fb of pp collision data in their search [18], finding no anomalous events. The experimental collaborations then give limits on heavy Majorana neutrinos in left-right (LR) symmetric models, derived from this data.

However, LNV searches at the LHC do not give bounds only for LR models. In principle, all models that contribute to eq.(1) via short-range contributions should lead to a LNV

[1] Neither in the long-range nor the short-range part of the amplitude the neutrino mass does appear directly. However, the $\Delta L = 2$ interactions, present necessarily in all contributions to $0\nu\beta\beta$ decay, implies Majorana neutrino masses must be non-zero in all possible models contributing to eq.(1) [4, 5].

[2] 14 events with an estimated background of 4 events [17], roughly equal to 2.8 σ c.l.

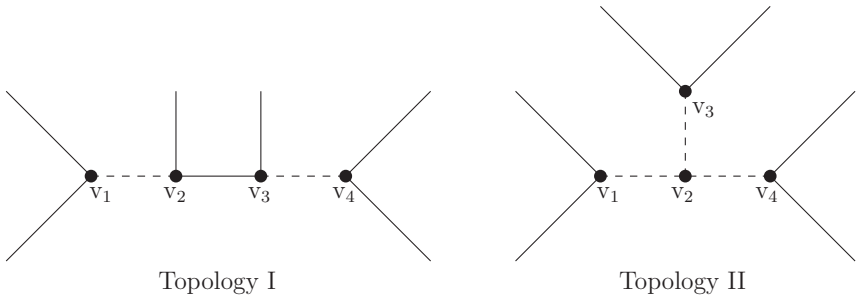

FIG. 1: *Tree-level topologies for the $d = 9$ $0\nu\beta\beta$ decay operator. External lines are fermions; internal lines can be fermions (solid) or scalars/vectors. For T-II there are in total 4 possibilities classified as: SSS, VVV, SSV and VVS. Only SSS and VVS can contribute significantly to $0\nu\beta\beta$ decay [8]. We will concentrate on scalar-only contributions.*

signal at the LHC. For the case of topology-I, the implications of LNV searches at the LHC and their connection to $0\nu\beta\beta$ decay has been studied in [19, 20]. In this paper we will study future LHC constraints on topology-II models. We will concentrate on the case where the non-SM particles are all scalars.

Both, ATLAS and CMS have published searches using dijets, based on $\sqrt{s} = 8$ TeV [21, 22] and $\sqrt{s} = 13$ TeV [23, 24] data. No new resonances have been observed in these searches, both collaborations give instead upper limits on $\sigma \times BR$ as a function of resonance mass. While dijet data of course can not be used to establish the existence of LNV, non-observation of new resonances in dijet searches at the LHC can be used to obtain limits on $0\nu\beta\beta$ decay [25]. In our analysis, presented below, we will also estimate the reach of future LHC data and compare it to expectations for the LNV searches.

As discussed below, in many of the models for T-II double beta decay leptoquarks (LQs) appear. Searches for leptoquarks have been carried out at the LHC by both ATLAS and CMS. Lower limits on the masses of first generation LQs from pair production in the $\sqrt{s} = 8$ TeV data are now roughly of the order of 1 TeV [26, 27]. ATLAS has published first limits from $\sqrt{s} = 13$ TeV data with only 3.2/fb, which already give very similar limits [28] despite the smaller statistics. Searches for singly produced LQs, published by CMS [29], give more stringent limits, albeit only for large values of the LQ coupling to quarks and leptons. Also these limits and results of future searches can be used to constrain short-range contributions to double beta decay and we take into account these constraints in our numerical analysis.

The rest of this paper is organized as follows. In section II we discuss different T-II contributions to $0\nu\beta\beta$ decay. We give the Lagrangian and necessary definitions for three example models. These models cover the optimistic/pessimistic cases for $0\nu\beta\beta$ decay. In section III, we present our numerical results. We then close with a short summary and discussion.

#	Decomposition	Mediator $(Q_{\rm em}, Q_{\rm colour})$ S	S'	S''
1	$(\bar{u}d)(\bar{u}d)(\bar{e}\bar{e})$	$(+1,\, \mathbf{1}$ or $\mathbf{8})$	$(+1,\, \mathbf{1}$ or $\mathbf{8})$	$(-2, \mathbf{1})$
2	$(\bar{u}d)(\bar{u}\bar{e})(\bar{e}d)$	$(+1,\, \mathbf{1}$ or $\mathbf{8})$	$(-1/3, \mathbf{3})$	$(-2/3, \overline{\mathbf{3}})$
3	$(\bar{u}\bar{u})(dd)(\bar{e}\bar{e})$	$(+4/3,\, \overline{\mathbf{3}}$ or $\mathbf{6})$	$(+2/3,\, \mathbf{3}$ or $\overline{\mathbf{6}})$	$(-2, \mathbf{1})$
4	$(\bar{u}\bar{u})(\bar{e}d)(\bar{e}d)$	$(+4/3,\, \overline{\mathbf{3}}$ or $\mathbf{6})$	$(-2/3, \overline{\mathbf{3}})$	$(-2/3, \overline{\mathbf{3}})$
5	$(\bar{u}\bar{e})(\bar{u}\bar{e})(dd)$	$(-1/3, \mathbf{3})$	$(-1/3, \mathbf{3})$	$(+2/3,\, \mathbf{3}$ or $\overline{\mathbf{6}})$

TABLE I: *List of decompositions for topology II from [8]. Only the electric and colour charges of the internal bosons are given here. All listed possibilities give short-range contributions. For the colour charges in some cases there exist two possible assignments.*

II. GENERAL SETUP

In this section we will first recall the general setup of the topology-II contributions to $0\nu\beta\beta$ decay. We will then give a few more details for those three concrete example models, that we will study numerically in section III. These examples, chosen from the full list of possible scalar models given in [8], allow us to cover both the most optimistic and the most pessimistic cases for the sensitivity of future double beta decay experiments.

A. Topology-II decompositions

Considering only the unbroken $SU(3)_C$ and $U(1)_Q$ there are only five possible decomposition of eq. (1) for topology-II. These are listed in table I. Note that in some cases there is more than one possibility for colour. There are six scalar states in these decompositions: (i) charged scalars, S^+ and S^{--}; (ii) diquarks, $S_{DQ}^{4/3}$ and $S_{DQ}^{2/3}$; and (iii) leptoquarks, $S_{LQ}^{-2/3}$ and $S_{LQ}^{-1/3}$.

Depending on the chirality of the outer fermions, the diquarks could come either from electro-weak (EW) singlets or triplets, while the leptoquarks could either be members of singlets or doublets. We have examples for each in the three selected models below. The singly charged scalar S^+ necessarily has to be a member of an $SU(2)_L$ doublet: $S_{1,2,1/2}$. Here and everywhere else in this paper the subscripts give the transformation properties under the SM group in the order $SU(3)_C \times SU(2)_L \times U(1)_Y$. Finally, S^{--} could either come from an EW singlet or a triplet.

Considering the full SM group, overall [8] gives 27 different combinations ("models") for the five decompositions shown in table I. All of these generate Majorana neutrino masses, from tree-level masses for decompositions with $S_{1,3,-1}$ to 4-loop neutrino masses for the diagram containing $S_{3,1,-1/3} - S_{3,1,-1/3} - S_{\bar{6},1,2/3}$ [4]. Our three examples correspond to two 2-loop and one 1-loop model, see below. This is motivated by the fact that for 2-loop neutrino mass models one can expect that the short-range part of the amplitude for $0\nu\beta\beta$

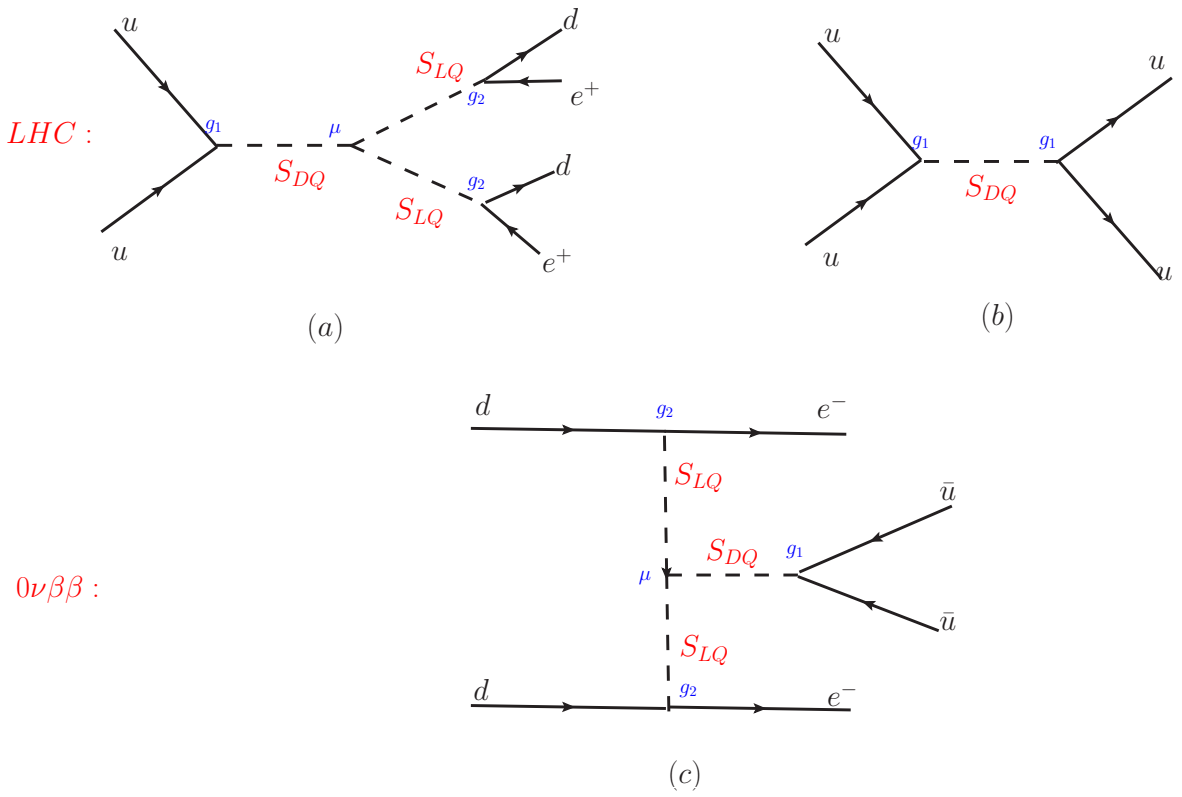

FIG. 2: Quark-level Feynman diagrams for (a) same-sign dilepton plus jets ($lljj$) signal, (b) dijet signal at the LHC and (c) neutrinoless double beta decay for the example model-1 containing a diquark and a leptquark scalar state.

and the mass mechanism can give similar contributions to the overall decay rate [4].

B. Selected example models

Here, we will give the basic Lagrangian terms of three decompositions of the $d = 9$ $0\nu\beta\beta$ decay operator taken from [8]. These examples correspond to T-II-2 BL # 11, T-II-4 BL # 11 and T-II-5 BL # 11 in the notation of [8]. Constraints on other short-range T-II decompositions will be very similar to these examples, as we will also discuss in section III.

1. T-II-4, BL # 11

Our first example model contains two new particles: A scalar diquarks and a leptoquark. In the context of $0\nu\beta\beta$ decay, diquark contributions were first discussed in [30]. We define scalar diquarks as particles coupling to a pair of same-type quarks. We choose the example T-II-4, BL # 11 in the notation of [8]. This model generates neutrino masses at 2-loop order [4], which means the TeV scale is the natural scale to fit to neutrino data. One expects therefore that this model is testable at the LHC. Note that a possible SU(5) embedding of

this model has been recently discussed in [31].

The new beyond the SM states in this model are:

$$S_{DQ} = S_{6,3,1/3} = \begin{pmatrix} S_{DQ}^{1/3} & S_{DQ}^{4/3} \\ S_{DQ}^{-2/3} & -S_{DQ}^{1/3} \end{pmatrix}, \quad S_{LQ} = S_{3,2,1/6} = \begin{pmatrix} S_{LQ}^{2/3} \\ S_{LQ}^{-1/3} \end{pmatrix}.$$

The interaction Lagrangian of the model is given by:

$$\mathcal{L}^{(1)}_{DQLQ} = \mathcal{L}_{SM} + g_1\ \bar{Q}\tau_2 \cdot \hat{S}_{DQ} \cdot Q^c + g_2\ \bar{L}\tau_2 \cdot S^\dagger_{LQ} \cdot d_R + \mu\ S^\dagger_{LQ}\tau_2 \cdot \hat{S}_{DQ} \cdot S^\dagger_{LQ} + \text{h.c.} \quad (2)$$

Here we introduced the notation $\hat{S}_{DQ} = S^{(6)}_{DQ,a}(T_{\bar{\mathbf{6}}})^a_{IJ}$, with $I, J = 1-3$ and the color triplet indexes and $a = 1-6$ the color sextet indexes. g_1 and g_2 are dimensionless Yukawas and μ has dimension of mass. The symmetric 3×3 matrices $T_{\mathbf{6}}$ and $T_{\bar{\mathbf{6}}}$ can be found in ref. [8]. Note that eq. (2) violates lepton number by two units.

The inverse half-life for $0\nu\beta\beta$ for the diagram of figure 2, is given by [8]:

$$T^{-1}_{1/2} = G_{01}\left|\epsilon_{DQ}\mathcal{M}_{DQ}\right|^2, \quad (3)$$

where G_{01} is a phase space integral and ϵ_{DQ} is defined by

$$\epsilon_{DQ} = \frac{2m_p}{G_F^2}\frac{g_1 g_2^2 \mu}{m^2_{DQ} m^4_{LQ}}, \quad (4)$$

and the nuclear matrix element is:

$$\mathcal{M}_{DQ} = \frac{1}{48}\mathcal{M}_1 - \frac{1}{192}\mathcal{M}_2. \quad (5)$$

Here $\mathcal{M}_{1,2}$ are defined in [3], numerical values for ^{136}Xe can be found in [1].

2. T-II-5, BL # 11

As a second example we discuss another model with a scalar diquark. However, this diquark couples only to down-type quarks. This model was first discussed in [32]. It corresponds to the example T-II-5, BL# 11 from the list of decompositions of the $d = 9$ $0\nu\beta\beta$ decay operator [8]. Also this model generates neutrino masses at 2-loop order as discussed in [4].

This particular case introduces a singlet diquark $S^{2/3}_{DQ} = S_{\bar{6},1,2/3}$ and a singlet leptoquark $S^{1/3}_{LQ} = S_{\bar{3},1,1/3}$. With these new fields, the Lagrangian contains the interactions:

$$\mathcal{L}^{(2)}_{DQLQ} = \mathcal{L}_{SM} + g_1\ \bar{d^c_R} \cdot \hat{S}^{2/3}_{DQ} \cdot d_R + g_2\ \bar{L}\tau_2 \cdot Q^c \cdot S^{1/3\,\dagger}_{LQ} + \mu\ S^{1/3\,\dagger}_{LQ} \cdot \hat{S}^{2/3}_{DQ} \cdot S^{1/3\,\dagger}_{LQ} + \text{h.c.}$$

Here, as before, by definition $\hat{S}^{2/3}_{DQ} = S^{2/3}_{DQ,a}(T_{\mathbf{6}})^a_{IJ}$.

The inverse half-life for the short-range $0\nu\beta\beta$ decay in this model has the same form as eq. (3) (with some obvious replacements). In particular, it depends in the same combination of nuclear matrix elements.

3. T-II-2, BL# 11

Finally, we will discuss a model with a singly charged scalar. We choose the example T-II-2, BL#11 from the list of [8]. This model generates neutrino masses at 1-loop order [4].

In this model, we add the following states to the SM particle content:

$$S_{1,2,1/2} = \begin{pmatrix} S^1 \\ S^0 \end{pmatrix}, \qquad S_{LQ} = S_{3,2,1/6} = \begin{pmatrix} S_{LQ}^{(2/3)} \\ S_{LQ}^{(-1/3)} \end{pmatrix}, \qquad S_{LQ}^{1/3} = S_{\bar{3},1,1/3}. \tag{6}$$

With these new fields, the relevant Lagrangian is:

$$\begin{aligned} \mathcal{L}_{S_1 LQ} \;=\; & \mathcal{L}_{SM} + g_1\, \bar{Q} \cdot S_{1,2,1/2} \cdot d_R + g_2\, \bar{Q} \tau_2 \cdot L^c \cdot S_{LQ}^{1/3\,\dagger} + g_3\, \overline{d_R}\, L \tau_2 \cdot S_{LQ} \\ & + \mu\, S_{1,2,1/2}^{\dagger} \cdot S_{LQ} \cdot S_{LQ}^{1/3} + \text{h.c.} \end{aligned}$$

The inverse half-life for $0\nu\beta\beta$ (short-range part of the amplitude) can be written as:

$$T_{1/2}^{-1} = G_{01} \left| \epsilon_{S_1} \mathcal{M}_{S_1} \right|^2, \tag{7}$$

where ϵ_{S_1} is given by

$$\epsilon_{S_1} = \frac{2 m_p}{G_F^2} \frac{g_1 g_2 g_3 \mu}{m_{S_1}^2 m_{LQ}^4}, \tag{8}$$

and the matrix element is given by:

$$\mathcal{M}_{S_1} = -\frac{1}{16} \mathcal{M}_1. \tag{9}$$

Again, for further definitions and numerical values see [1, 3].

III. NUMERICAL RESULTS

In this section we present our numerical results. We estimate the sensitivity of current and future $0\nu\beta\beta$ experiments and compare them with the sensitivity of dijet, leptoquark and dilepton plus jets searches at LHC at $\sqrt{s} = 13$ TeV. For definiteness we assume two values for the accumulated luminosity $\mathcal{L}$: $\mathcal{L} = 20/\text{fb}$ and $\mathcal{L} = 300/\text{fb}$.

For the calculation of the cross sections of the diquark scalar resonances we use MadGraph5 [33], for the leptoquark and the singly charged scalar CalcHEP [34]. We have compared our results with the literature [35] and found good agreement with published values, whenever available. Plots for the cross sections can be found in our previous work on T-I contributions for $0\nu\beta\beta$ decay [20].

From the cross sections we then estimate the future LHC sensitivity as follows. For the LNV signal (lljj) we first take a simple fit [20] to the background of existing data of the CMS analysis [36] based on 3.6 fb^{-1} at $\sqrt{s} = 8$ TeV. We checked this fit against the CMS analysis [17] based on 19.7 fb^{-1} of data at $\sqrt{s} = 8$ TeV, published later, and found

good overall agreement. In the CMS analysis [17] the main background can be traced to $t\bar{t}$ events. We then do a simple estimate which considers that the $t\bar{t}$ production cross section is very roughly about a factor 3 higher at $\sqrt{s} = 13$ TeV than at $\sqrt{s} = 8$ TeV. Thus, we scale the original fit to $\sqrt{s} = 8$ TeV data with a simple constant and scale the background function from $\mathcal{L} = 3.6$ fb^{-1} to future expected luminosities of $\mathcal{L} = 20$/fb and 300/fb. For the estimation of the future dijet background we use the fit of the SM dijet distribution fitted to Monte Carlo simulation given in [37]. For both, dijet and $lljj$ analysis we then estimate backgrounds as dicussed above and define the sensitivity reach as either the simple square root of the background (times two for 95 % c.l.) or 5 signal events, whichever is larger. For future LQ searches at the LHC, we calculate LQ pair production cross sections as a function of LQ mass. We simply define the reach of the LQ search then as the mass for which there are less then 10 signal events in 20/fb (300/fb) at the LHC (before cuts). This results in the simple estimate of $m_{LQ} \gtrsim 1.3$ TeV ($m_{LQ} \gtrsim 1.8$ TeV) as the near (far) future limit. Thus, our results should be considered only rough estimates. For more exact results a full MonteCarlo simulation including detector effects would be necessary.

For double beta decay we use the current limit of $T_{1/2}^{0\nu\beta\beta}(^{136}Xe) \geq 1.1 \times 10^{26}$ yr from the KamLAND-Zen collaboration [7].[3] Several experimental proposals aim at half-life sensitivities of the order of 10^{27} yr. We will use the estimated sensitivity of the nEXO proposal [40, 41] of $T_{1/2}^{0\nu\beta\beta}(^{136}Xe) \simeq 6 \times 10^{27}$ yr for our calculation of the future limits. We convert half-life limits into limits on masses and couplings, using the equations discussed in the previous section. We take into account the QCD corrections to the Wilson coefficients, calculated recently in [42]. In particular for the model with the singly charged scalar QCD corrections have been found to be very important numerically.

We will first discuss the case of our example model 1, see the Lagrangian in eq. (2). In this model the three components of the triplet diquark, the scalars $S_{DQ}^{(4/3)}, S_{DQ}^{(1/3)}, S_{DQ}^{(-2/3)}$, contribute to the dijet cross section. However, the dominant contribution to the dijet cross section comes from the diquark scalar $S_{DQ}^{(4/3)}$. The Feynman diagram is shown in fig. 2. We have assumed for simplicity that the Yukawa couplings g_1 and g_2 are different from zero for the first quark and lepton generations only. As is shown in fig. 2, the scalar diquark $S_{DQ}^{(4/3)}$ can only decay through two possible channels: dijets (jj) and dilepton plus two jets (lljj). The respective branching ratios can be calculated directly from the Lagrangian (2) and are a function of the leptoquark mass m_{LQ} and the (unknown) parameters μ and g_2.

In Fig. 3 we show a comparison between $0\nu\beta\beta$ decay and dijet, LQ and dilepton plus jets searches at LHC in the plane m_{DQ} vs m_{LQ}, for two fixed choice of $g_1 = g_2$ (bottom: $g_1 = g_L$, top: $g_1 = 0.2$) and two values for the accumulated luminosity: $\mathcal{L} = 20$/fb (left) and $\mathcal{L} = 300$/fb (right). Here, g_L is the $SU(2)_L$ coupling. μ is chosen as $\mu = m_{DQ}/6$ (bottom) and $\mu = m_{DQ}$ (top). The vertical black line corresponds to future limits from dijet searches at the LHC, the horizontal purple line is for leptoquark searches and the triangular red curve

[3] For the mass mechanism this limit corresponds to $\langle m_\nu \rangle \lesssim 0.1$ (0.14) eV, depending on nuclear matrix elements [38] ([39]).

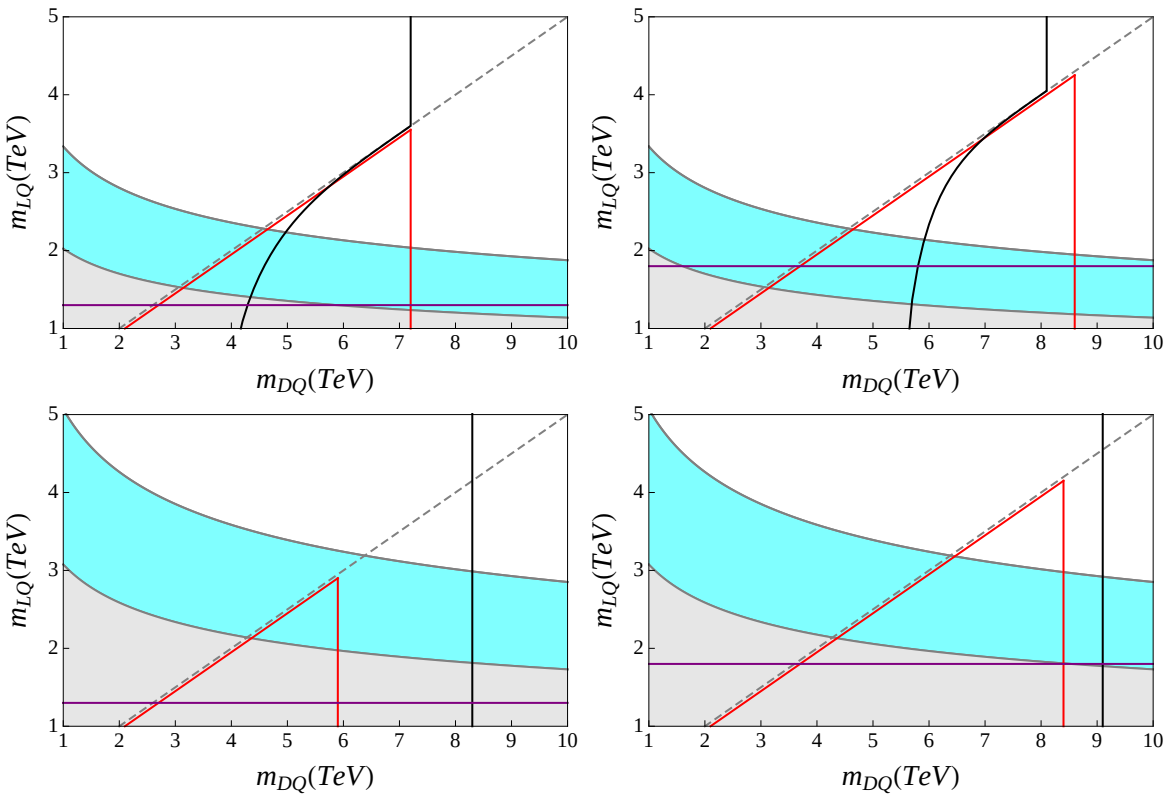

FIG. 3: Expected future sensitivities for the LHC at $\sqrt{s} = 13$ TeV, $\mathcal{L} = 20$/fb (left) and $\mathcal{L} = 300$/fb (right), compared with current and future double beta decay experiments for the diquark model described in the Lagrangian eq. (2). The vertical black line corresponds to future limits coming from dijet searches at the LHC, the horizontal purple line from leptoquark searches and the triangular red curve covers the region for like sign leptons plus two jets search. We use the parameters $g_1 = g_2 = g_L$ (bottom) and $g_1 = g_2 = 0.2$ (top). μ is taken as $\mu = \frac{m_{DQ}}{6}$ (bottom) and $\mu = m_{DQ}$ (top). The gray region corresponds to the current lower limit for the $0\nu\beta\beta$ decay half-life of ^{136}Xe, the blue one corresponds to the estimated future sensitivity of $T_{1/2} = 6 \times 10^{27}$ ys of the nEXO proposal. The dashed line marks the kinematic limit for the $lljj$ search, where $m_{DQ} = 2 \times m_{LQ}$. For more details see text.

covers the region probed by the $lljj$ search. The dashed line shows the kinematic limit for the $lljj$ signal, where $m_{DQ} = 2 \times m_{LQ}$. For masses $m_{DQ} < 2 \times m_{LQ}$, one of the LQs goes off-shell and the branchig ratio for the final state $lljj$ drops to unmeasurably small values.

As the figs (3) on the left show, LHC searches will significantly constrain parameter regions of LNV models contributing to $0\nu\beta\beta$ decay already with moderate luminosities. The $lljj$ signal depends very sensitively on the choice of μ, while the dijet signal depends mostly on the value of g_1. Smaller values of μ reduce the branching ratio for the $lljj$ final state, reducing its reach. However, in this case the branching ratio for the dijet final states increases, making the dijet search more powerful, as the figure shows. We stress again, that while dijet searches can be used to exclude parameter regions of LNV models contributing

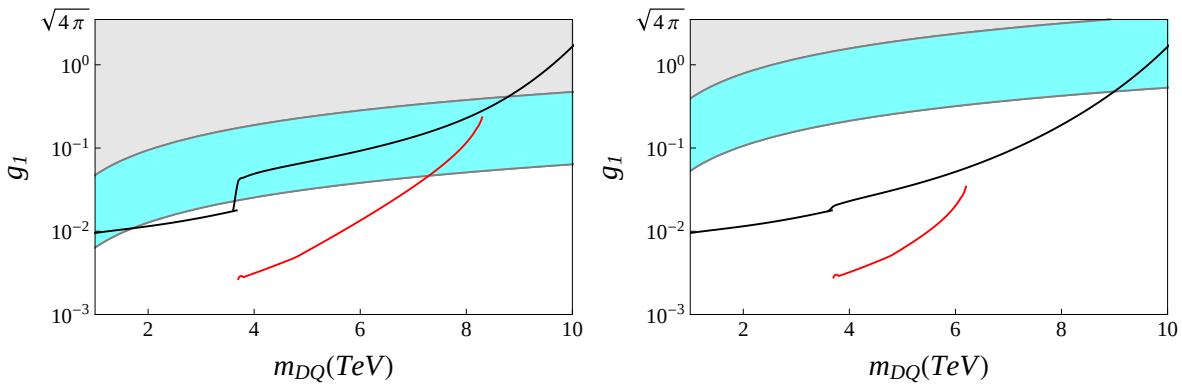

FIG. 4: Regions in parameter space of the diquark model described in the Lagrangian (2), which can be probed by dijet (black curves) and like sign leptons plus two jets (red curves) searches at LHC at $\sqrt{s} = 13$ TeV and $\mathcal{L} = 300$ fb^{-1}. We use the parameters $m_{LQ} = 1.8$ TeV, $g_2 = g_L$, $\mu = \frac{m_{DQ}}{6}$ (left) and $\mu = \frac{m_{DQ}}{50}$ (right). The gray region is the current lower limit in $0\nu\beta\beta$ decay half-life, the blue one the estimated future sensitivity of $T_{1/2} = 6 \times 10^{27}$ ys. For more details see text.

to $0\nu\beta\beta$ decay, to establish a direct relation between $0\nu\beta\beta$ and LHC, a positive result from the LNV search ($lljj$) at the LHC would be necessary.

For $\mathcal{L} = 300$/fb, see fig. (3) on the right, the LHC can probe up to DQ masses of the order of $8 - 9$ TeV (for $g_1 \geq 0.2$). Whether dijet or LNV signal are more constraining depends on the exact value of μ We have chosen the value of $\mu = m_{DQ}/6$, because, as the figure on the bottom right shows, negative results from LHC LQ and dijet searches would rule out partial $0\nu\beta\beta$ decay half-lives in this model below the current experimental limit for $\mu = m_{DQ}/6$, assuming $g_1 = g_2 = g_L$. For $\mu \leq m_{DQ}/50$ negative searches from the LHC would rule out partial $0\nu\beta\beta$ decay half-lives below the future bound of $T_{1/2} = 6 \times 10^{27}$ ys.

$0\nu\beta\beta$ decay depends on the mean of the couplings and masses, see eq. (4). Thus, in general LHC and $0\nu\beta\beta$ decay probe complementary parts of parameter space. This can also be seen in fig. (3): For large values of μ and/or large values of g_1 and g_2 there is always a region in parameter space for large values of the DQ mass, where double beta decay is more sensitive than the LHC.

In Fig. 4 we show the comparison between the $0\nu\beta\beta$ decay and dijet and dilepton plus jets searches at LHC in the plane $g_1 - m_{DQ}$. The LQ mass was chosen as $m_{LQ} = 1.8$ TeV, roughly the expected future bound from LHC. $g_2 = g_L$, $\mu = \frac{m_{DQ}}{6}$ (left) and $\mu = \frac{m_{DQ}}{50}$ (right). Grey and blue regions show again the sensitivity of $0\nu\beta\beta$ decay current and future. The solid lines correspond to future LHC limits from dijet (black curves) and dilepton plus jets (red curves). The red curves start at $m_{DQ} = 2 \times m_{LQ}$ and stop at masses of the DQ, for which there are less than 5 signal events expected in $\mathcal{L} = 300$ fb^{-1}.

For these choices of parameters, dijet searches can probe larger masses, but the $lljj$ search probes smaller values of the coupling g_1. Again, for larger choices of μ the branching ratio for the $lljj$ final state is larger and the $lljj$ search becomes more sensitive. Negative

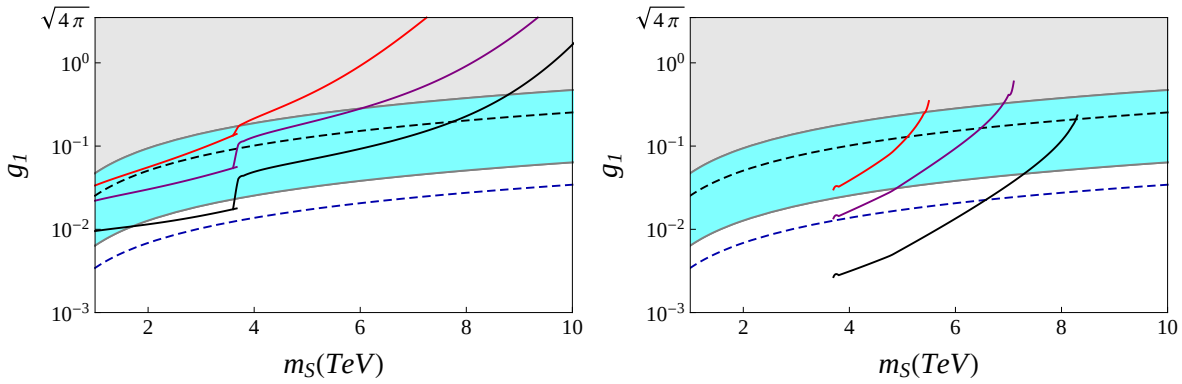

FIG. 5: Future limits for the LHC at $\sqrt{s} = 13$ TeV and $\mathcal{L} = 300$ fb^{-1} compared with current and future double beta decay experiments. The gray region is the current lower limit in $0\nu\beta\beta$ decay half-life whereas the blue region represents the parameter region accessible in near future $0\nu\beta\beta$ experiments. The colored lines shows sensitivity limits for the LHC for dijet (left) and dilepton plus jets (right) searches for production of three different scalar bosons S_{+1}(red), $S^{DQ}_{2/3}$ (purple) and $S^{DQ}_{4/3}$ (black). These limits were calculated using $g_2 = g_L$ and $m_{LQ} = 1.8$ TeV and $\mu = \frac{m_{DQ}}{6}$. For more details see text.

results from the dijet searches would exclude large part of the parameter space explorable by future $0\nu\beta\beta$ decay experiments. However, for large values of μ there is always a corner of parameter space for large couplings and DQ masses, where $0\nu\beta\beta$ decay is more sensitive.

Finally in Fig. 5 we plot a comparison of sensitivities of $0\nu\beta\beta$ decay and the dilepton plus jets (Fig. 5 right) and dijet (Fig. 5 left) searches at LHC for the three different models discussed in section II: T-II-2 BL # 11 (singly charged scalar), T-II-4 BL # 11 (triplet diquark) and T-II-5 BL # 11 (singlet diquark). The double beta decay and LHC limits were calculated using the parameters $\mu = m_{DQ}/6$, $m_{LQ} = 1.8$ TeV and $g_2 = g_L$. The LHC is most sensitive for the case of the triplet diquark model (T-II-2 BL # 11), black curve. This is simply because the cross section of the resonance production of the scalar diquark $S^{(4/3)}_{DQ}$ is larger than the one for the diquark $S^{(-2/3)}_{DQ}$ (purple curve) and the singled charged scalar S^1 (red curve). Fig. 5 shows also current and future limits from $0\nu\beta\beta$ decay for the respective models in consideration. The gray area is the currently excluded part of parameter space from non observation of ^{136}Xe decay with $T_{1/2} > 1.1 \times 10^{26}$ yr and the blue one the estimated future sensitivity, as before. The full lines are for the two diquark models (which have the same nuclear matrix elements, see above). The dashed lines are for the singly charged scalar model (T-II-2 BL # 11), which has a different nuclear matrix element, compare eqs (5) and (9). LHC is least sensitive for the singly charged scalar case, the $S^{(-2/3)}_{DQ}$ is intermediate between the other two.

Finally, we briefly comment on other T-II models. As shown in table I, all T-II decompositions contain either a diquark or a charged scalar (in one case two different diquarks). The three example models, which we used in the numerical analysis, covers the cases with the largest and smallest cross sections at the LHC. It also covers the models with the largest and

smallest matrix elements for the $0\nu\beta\beta$ decay. Thus, our sensitivity estimate for the future covers the extreme cases, both optimistic and pessimistic, and all other models should lie somewhere in between.

In case of a discovery in the future at the LHC, one important question to ask is, which of the different model possibilities is the one realized in nature. As in the case of T-I [20], this might be achieved by investigating mass peaks in different variables and by the measurememt of the "charge asymmetry", i.e. the measurement of the number of events in l^-l^-jj relative to l^+l^+jj.

IV. DISCUSSION AND SUMMARY

We have discussed how future LNV and dijet searches at the LHC can be used to constrain scalar short-range contributions to neutrinoless double beta decay (topology-II diagrams). We have concentrated on three LNV models, chosen from the full list of possible scalar short-range contributions to $0\nu\beta\beta$ decay given in [8]. Two of these models contribute to $0\nu\beta\beta$ decay through short-range diagrams mediated by diquark scalars and one of them by a singly charged scalar. For these models we have shown that the future LNV and dijet searches at the LHC will provide stringent constraints on the parameter space of the models, complementary to $0\nu\beta\beta$ decay experiments. Except for small parts of the parameter region of these LNV models, a $0\nu\beta\beta$ decay signal corresponding to a half life in the range $T_{1/2} < 10^{27}$ ys should imply a positive LNV or dijet signal at the LHC. On the other hand, the non-observation of a positive signal at the LHC would rule out most of the parameter region measurable in $0\nu\beta\beta$ decay. We note that, while we have concentrated on three particular examples, similar constraints will apply to any scalar short-range contributions to $0\nu\beta\beta$.

Finally, we mention that the observation of lepton number violation at the LHC and/or in double beta decay will have important consequences for high-scale models of leptogenesis [43, 44].

Acknowledgements

This work was supported by the Spanish grants FPA2014-58183-P, Multidark CSD2009-00064 and SEV-2014-0398 (from the *Ministerio de Economía y Competitividad*), as well as PROMETEOII/2014/084 (from the *Generalitat Valenciana*). J.C.H. is supported by Chile grants Fondecyt No. 1161463, Conicyt ACT 1406 and Basal FB0821. L. G. is supported by Conicyt (Chile) under Grant No. 21160645 and by the DGIP of the UTFSM. S. K. is supported by FONDECYT (Chile) grant No. 1150792, CONICYT (Chile) Ring ACT 1406 and Basal FB0821.

[1] F. F. Deppisch, M. Hirsch, and H. Päs, J.Phys. **G39**, 124007 (2012), arXiv:1208.0727.

[2] H. Päs, M. Hirsch, H. Klapdor-Kleingrothaus, and S. Kovalenko, Phys.Lett. **B453**, 194 (1999).
[3] H. Päs, M. Hirsch, H. Klapdor-Kleingrothaus, and S. Kovalenko, Phys.Lett. **B498**, 35 (2001), arXiv:hep-ph/0008182.
[4] J. Helo, M. Hirsch, T. Ota, and F. A. P. Dos Santos, JHEP **1505**, 092 (2015), arXiv:1502.05188.
[5] J. C. Helo, M. Hirsch, and T. Ota, JHEP **1606**, 006 (2016), arXiv:1602.03362.
[6] GERDA Collaboration, M. Agostini et al., Phys.Rev.Lett. **111**, 122503 (2013), arXiv:1307.4720.
[7] KamLAND-Zen, A. Gando et al., (2016), arXiv:1605.02889.
[8] F. Bonnet, M. Hirsch, T. Ota, and W. Winter, JHEP **1303**, 055 (2013), arXiv:1212.3045.
[9] R. N. Mohapatra and G. Senjanovic, Phys. Rev. **D23**, 165 (1981).
[10] R. N. Mohapatra, Phys.Rev. **D34**, 909 (1986).
[11] M. Hirsch, H. Klapdor-Kleingrothaus, and O. Panella, Phys.Lett. **B374**, 7 (1996), arXiv:hep-ph/9602306.
[12] W.-Y. Keung and G. Senjanovic, Phys.Rev.Lett. **50**, 1427 (1983).
[13] S. Das, F. Deppisch, O. Kittel, and J. Valle, (2012), arXiv:1206.0256.
[14] G. Bambhaniya, J. Chakrabortty, J. Gluza, T. Jelinski, and R. Szafron, Phys. Rev. **D92**, 015016 (2015), arXiv:1504.03999.
[15] P. S. B. Dev, R. N. Mohapatra, and Y. Zhang, JHEP **05**, 174 (2016), arXiv:1602.05947.
[16] M. Lindner, F. S. Queiroz, and W. Rodejohann, (2016), arXiv:1604.07419.
[17] CMS, V. Khachatryan et al., Eur. Phys. J. **C74**, 3149 (2014), arXiv:1407.3683.
[18] ATLAS, G. Aad et al., JHEP **07**, 162 (2015), arXiv:1506.06020.
[19] J. Helo, M. Hirsch, S. Kovalenko, and H. Päs, Phys.Rev. **D88**, 011901 (2013), arXiv:1303.0899.
[20] J. Helo, M. Hirsch, H. Päs, and S. Kovalenko, Phys.Rev. **D88**, 073011 (2013), arXiv:1307.4849.
[21] ATLAS, G. Aad et al., Phys.Rev. **D91**, 052007 (2015), arXiv:1407.1376.
[22] CMS, V. Khachatryan et al., Phys.Rev. **D91**, 052009 (2015), arXiv:1501.04198.
[23] ATLAS, G. Aad et al., Phys. Lett. **B754**, 302 (2016), arXiv:1512.01530.
[24] CMS, V. Khachatryan et al., Phys. Rev. Lett. **116**, 071801 (2016), arXiv:1512.01224.
[25] J. C. Helo and M. Hirsch, Phys. Rev. **D92**, 073017 (2015), arXiv:1509.00423.
[26] CMS, V. Khachatryan et al., Phys. Rev. **D93**, 032004 (2016), arXiv:1509.03744.
[27] ATLAS, G. Aad et al., Eur. Phys. J. **C76**, 5 (2016), arXiv:1508.04735.
[28] ATLAS, M. Aaboud et al., (2016), arXiv:1605.06035.
[29] CMS, V. Khachatryan et al., Phys. Rev. **D93**, 032005 (2016), arXiv:1509.03750.
[30] P.-H. Gu, Phys.Rev. **D85**, 093016 (2012), arXiv:1101.5106.
[31] R. M. Fonseca and M. Hirsch, Phys. Rev. **D92**, 015014 (2015), arXiv:1505.06121.
[32] M. Kohda, H. Sugiyama, and K. Tsumura, Phys.Lett. **B718**, 1436 (2013), arXiv:1210.5622.
[33] J. Alwall et al., JHEP **1407**, 079 (2014), arXiv:1405.0301.
[34] A. Pukhov, (2004), arXiv:hep-ph/0412191.
[35] T. Han, I. Lewis, and Z. Liu, JHEP **1012**, 085 (2010), arXiv:1010.4309.
[36] CMS, (2012), CMS-PAS-EXO-12-017.

[37] P. Richardson and D. Winn, Eur. Phys. J. **C72**, 1862 (2012), arXiv:1108.6154.

[38] F. Šimkovic, V. Rodin, A. Faessler, and P. Vogel, Phys. Rev. **C87**, 045501 (2013), arXiv:1302.1509.

[39] K. Muto, E. Bender, and H. Klapdor, Z.Phys. **A334**, 187 (1989).

[40] A. Pocar, PoS **NEUTEL2015**, 049 (2015).

[41] A. Pocar, Nucl. Part. Phys. Proc. **265-266**, 42 (2015).

[42] M. González, M. Hirsch, and S. G. Kovalenko, Phys. Rev. **D93**, 013017 (2016), arXiv:1511.03945.

[43] F. F. Deppisch, J. Harz, and M. Hirsch, Phys.Rev.Lett. **112**, 221601 (2014), arXiv:1312.4447.

[44] F. F. Deppisch, J. Harz, M. Hirsch, W.-C. Huang, and H. Päs, Phys. Rev. **D92**, 036005 (2015), arXiv:1503.04825.